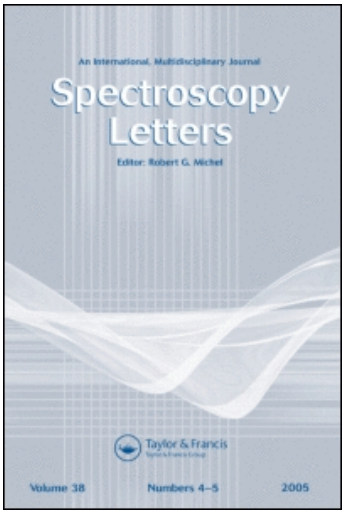

Spectroscopy Letters
Publication details, including instructions for authors and subscription information:
http://www.informaworld.com/smpp/title~content=t713597299

Sequence and Hot Transitions in the Co_2 Molecule; Interference of Adjacent Lines Belonging to Different Transitions as a Function of Temperature

Ljubica T. Petkovska[a]
[a] Department of Physical Chemistry, Vinca Institute of Nuclear Sciences, Belgrade, F.R., Yugoslavia

To cite this Article Petkovska, Ljubica T.(2000) 'Sequence and Hot Transitions in the Co_2 Molecule; Interference of Adjacent Lines Belonging to Different Transitions as a Function of Temperature', Spectroscopy Letters, 33: 3, 283 — 300
To link to this Article: DOI: 10.1080/00387010009350077
URL: http://dx.doi.org/10.1080/00387010009350077

SPECTROSCOPY LETTERS, 33(3), 283–300 (2000)

SEQUENCE AND HOT TRANSITIONS IN THE CO_2 MOLECULE; INTERFERENCE OF ADJACENT LINES BELONGING TO DIFFERENT TRANSITIONS AS A FUNCTION OF TEMPERATURE

Key words: IC- spectroscopy, CO_2, CO_2-laser, photoacoustic

Ljubica T. Petkovska

Vinca Institute of Nuclear Sciences, Department of Physical Chemistry
POB 522, 11001 Belgrade, F.R. Yugoslavia,
E-mail: ljubicap@rt270.vin.bg.ac.yu

ABSTRACT

Carbon-dioxide spectra of some higher transitions in the 9-11μm region were studied. Spectra of the sequence ($[10^01,02^01]_{I,II}$ - 00^02) and hot (01^11 - 11^10) bands were calculated as a function of temperature. The positions of the ro-vibrational transitions and their intensities were determined as a function of temperature. For lines in hot and sequence transitions whose positions are close to some of the regular lines $([10^00,02^00]_{I,II}$ - $00^01)^1$ absorption coefficients of adjacent lines were calculated as functions of line center distances and temperature. The resulting values of the absorption coefficient for conditions of constant pressure or constant volume were determined.

INTRODUCTION

The CO_2-laser oriented spectroscopy usually recognizes the so-called "regular", sequence, and "hot" bands in either emission or absorption in the area of CO_2-laser emission. CO_2 emission includes two bands centered at 9.4 μm and 10.4μm, which are the result of transitions from vibrational level 00^01 to two lower levels, 10^00 and 02^00. (Fig.1).

In laser spectroscopy these bands are called "regular". The sequence bands are upper analogues of the regular ones, since they correspond to transitions $[10^01,02^01]_{I,II}$ - 00^02 (first sequence), then to $[10^02,02^02]_{I,II}$ - 00^03, and so on. "Hot" bands (11^10 - 01^11) are not regular nor sequence but bands that correspond to other kinds of transitions between carbon-dioxide vibrational levels. Their wavelength region partially overlaps with the corresponding region of the regular bands.

All CO_2 absorption bands that appear in the CO_2-laser emission range are relatively weak, being the result of transitions between the higher (not fundamental) vibrational levels that are poorly populated at room temperature. With increasing temperature higher levels become more populated, which changes the relative intensities of absorption (or emission) associated with transitions appearing in this region. Investigations of carbon dioxide absorption at elevated temperatures are interesting due to several reasons. Knowing the temperature dependence of absorption for some transitions has made possible the realization of the laser emission with transition ($[10^01,02^01]_{I,II}$ - 00^02), i.e. the first sequence bands, and obtaining the so-called sequence laser[2-4], which also includes the 9-11 μm region, but with shifted wavelengths with respect to the regular CO_2-laser. There is a CO_2 band of a much higher intensity than the sequence bands, called the hot band (although all of these could be called hot transitions), which only partially overlaps the CO_2 emission. This transition would probably also be interesting as potential laser emission, provided that a possibility is found for obtaining population inversion within ($11^10 \rightarrow 01^11$). The analysis given in the present paper should contribute to better understanding and

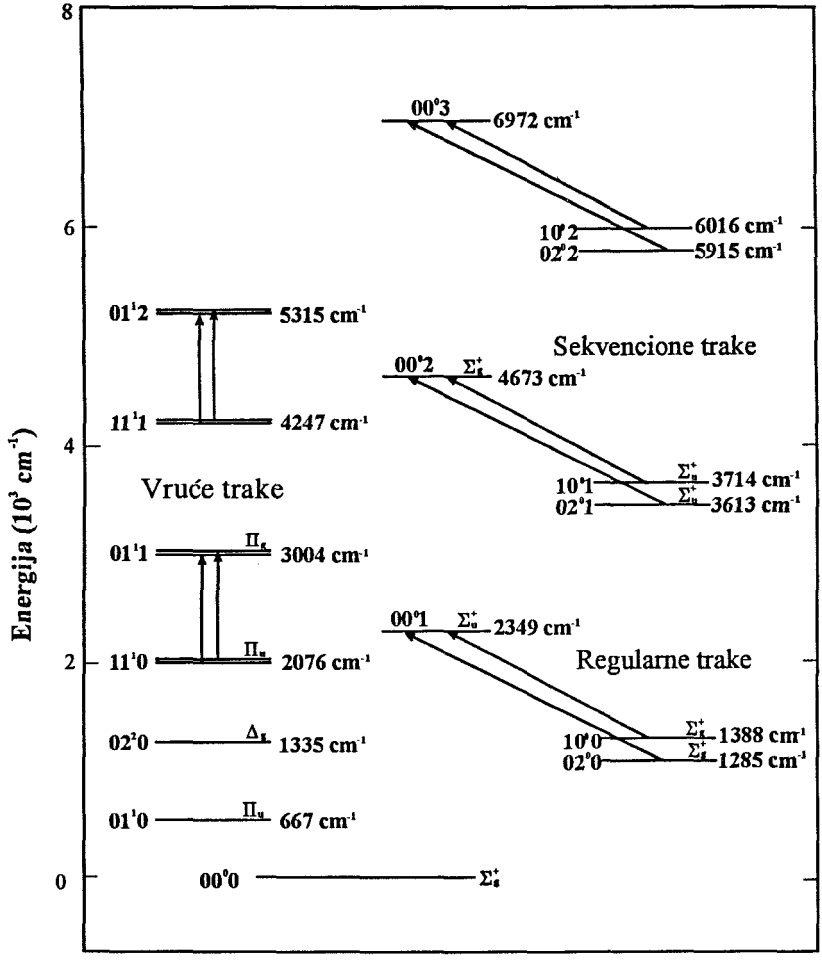

Figure 1. Simplified vibrational energy level diagram of carbon-dioxide

elucidation of the details of carbon-dioxide spectroscopy, as well as interpretation of experimental photoacoustic spectroscopy data[1]. Line positions, intensities and absorption coefficients of sequence and hot bands are considered. The overlapping of absorption lines belonging to different transitions with adjacent positions was treated via the sum absorption coefficient.

THEORETICAL CONSIDERATION

A partial energy map of the CO_2 ro-vibrational transitions is given in Fig. 1. Besides the "regular" bands, for which the results are mainly published in the previous paper[1], the first sequence band-set (transitions $[10^01,02^01]_{I,II}$ - 00^02) and the hot band ($11^10 \rightarrow 01^11$) are considered here. Only these bands are worth considering, because they have comparable values of line intensities to those in the regular bands and some of their lines are sufficiently close to lines in the regular band[1]. Other higher transitions, also appearing in this region, are not considered, due to their low population at temperatures under study.

Wavenumbers of the ro-vibrational line centers (in cm^{-1}) in all the bands were calculated for transitions from a lower (") to a higher (') energy level[5]

$$\nu_0 = \nu_v + (B' + B'')m + (B' - B''-D' + D'')m^2 - 2(D' + D'')m^3 - (D' - D'')m^4 \qquad (1)$$

where ν_v is the band origin obtained as the difference between the corresponding vibrational states; B' and B'' are the rotational (inertia) constants, and D' and D'' are centrifugal distortion constants of the molecule in the upper and the lower state, respectively; m=-J when J'=J-1 (P-branch), or m=J+1 when J'=J+1 (R-branch). J is the rotational quantum number in the lower state.

$$\nu_0 = \nu_v + (B' - B'')J(J+1) - (D' - D'')J^2(J+1)^2 \qquad (2)$$

The corresponding equation for the the Q-branch (ΔJ=0), appearing only in hot transitions of this region, is given as: The interaction of rotation with vibration is manifested through the rotational constants being slightly different for different vibrational levels. All the data necessary for the calculation are given in ref.[1,6]

The spectral line intensity, or, the integrated absorption coefficient, is given by the relation[7]

$$S = \int_{-\infty}^{\infty} k(\nu)d\nu; \qquad k(\nu) = S \cdot f(\nu - \nu_0); \qquad \int_{-\infty}^{\infty} f(\nu - \nu_0) = 1 \qquad (3)$$

where $k(\nu)$ is the absorption coefficient as defined by Lambert-Beer's law [8], $f(\nu - \nu_0)$ is the so-called "shape" function of the spectral line, and ν_0 the line center wavelength.

The integrated intensity of absorption, S [cm^{-2} $mbar^{-1}$], can be obtained as:

$$S = \frac{8\pi^3}{3hc}\nu_0 \frac{n}{Q(T)} e^{-\frac{hc}{kT}E''} [1 - e^{-\frac{hc}{kT}\nu_0}] S_{HL} |R|^2 \qquad (4)$$

where h is the Planck's constant, c is the speed of light, k is the Boltzmann's constant, S_{HL} is Hönle-London's factor and $|R|$ is the dipole moment matrix element of the corresponding transition, n is the total number of molecules of the absorbing gas per pressure and volume units, E'' is the lower energy state, $Q(T)$ is the total partition function of the molecule. In the ideal gas state the total partition function is equal to its internal part, in our case - vibration/rotational transitions.

It follows from equation (3) that the absorption coefficient can be calculated if the integrated intensity of absorption, eqn. (4), and shape function are obtained for the corresponding conditions. The shape function values can be obtained assuming the Lorentz (collisional) mechanism of line broadening (predominant above 50 Torr) as:

$$f(\nu - \nu_0) = \frac{b_L}{\pi[(\nu - \nu_0)^2 + b_L^2]}. \qquad (5)$$

The Lorentz half-width, b_L, defined as one half the full width at half maximum (HWHM).

RESULTS AND DISCUSSION

Table 1 contains the calculated wavelength positions of the ro-vibrational lines of the sequence bands $[10^01,02^01]_{I,II}$ - 00^02). The corresponding values for the regular bands are given in the previous paper [1].

Table 1. Calculated wavenumbers at 600K of CO_2 sequence bands

Line	Wavenumber [cm^{-1}]	Line	Wavenumber [cm^{-1}]	Line	Wavenumber [cm^{-1}]	Line	Wavenumber [cm^{-1}]
10^01 -00^02		10^01 -00^02		02^01 - 00^02		02^01 - 00^02	
R(1)	960.0830	P(1)	957.7788	R(1)	1062.0244	P(1)	1059.7202
R(3)	961.5896	P(3)	956.2126	R(3)	1063.5264	P(3)	1058.1494
R(5)	963.0718	P(5)	954.6226	R(5)	1065.0005	P(5)	1056.5513
R(7)	964.5300	P(7)	953.0085	R(7)	1066.4475	P(7)	1054.926
R(9)	965.9641	P(9)	951.3708	R(9)	1067.8665	P(9)	1053.2732
R(11)	967.3738	P(11)	949.7087	R(11)	1069.2578	P(11)	1051.5928
R(13)	968.7598	P(13)	948.0229	R(13)	1070.6221	P(13)	1049.8853
R(15)	970.1211	P(15)	946.3135	R(15)	1071.9585	P(15)	1048.1509
R(17)	971.4580	P(17)	944.5796	R(17)	1073.2676	P(17)	1046.3892
R(19)	972.7705	P(19)	942.8218	R(19)	1074.5491	P(19)	1044.6003
R(21)	974.0588	P(21)	941.0398	R(21)	1075.8040	P(21)	1042.7849
R(23)	975.3223	P(23)	939.2344	R(23)	1077.0310	P(23)	1040.9431
R(25)	976.5608	P(25)	937.4045	R(25)	1078.2307	P(25)	1039.0745
R(27)	977.7747	P(27)	935.5500	R(27)	1079.4036	P(27)	1037.179
R(29)	978.9636	P(29)	933.6716	R(29)	1080.5496	P(29)	1035.2576
R(31)	980.1274	P(31)	931.7690	R(31)	1081.6685	P(31)	1033.3101
R(33)	981.2661	P(33)	929.8418	R(33)	1082.7610	P(33)	1031.3367
R(35)	982.3799	P(35)	927.8906	R(35)	1083.8267	P(35)	1029.3374
R(37)	983.4683	P(37)	925.9146	R(37)	1084.8662	P(37)	1027.3125
R(39)	984.5303	P(39)	923.9141	R(39)	1085.8789	P(39)	1025.2627
R(41)	985.5669	P(41)	921.8887	R(41)	1086.8657	P(41)	1023.1875

The sequence bands considered here are the result of the transition ($[10^01$, $02^01]_{I,II}$ - 00^02), which is a $\Sigma_u^+ \rightarrow \Sigma_g^+$ transition (Fig. 1). They only contain odd rotational lines (since the rotational quantum number J of the lower Σ_u^+ state in CO_2 can only have odd values). The range of wavelengths covered by the sequence bands is practically the same as the range of the regular bands, but line positions are different.

Table 2 presents the calculated values of the positions of the (11^10-01^11) hot band lines. This transition belongs to Π_u - Π_g transitions that are characteristic[5] of producing double lines for each *J*, whose positions differ very little, and whose intensities are very similar for $D_{\infty h}$ symmetry molecules, such as CO_2. These doublets originate from double levels within the Π states for each *J*. Labels "D" and "C" in Table 2 refer to 11^10C - 01^11C, and 11^10D - 01^11D transitions respectively, where the "C" levels[6, 14, 15] are Σ^+ levels for even *J*, and Σ^- levels for odd *J*. The opposite is valid for the "D" values. In the present case transition rule[s] give: D - D and C - C for $\Delta J=\pm 1$ (R and P branch) and D - C for $\Delta J=0$ (Q branch). It follows from Table 2 that the lines of the hot transition under study range from 10.5 to 11.3 μm, and only partly overlap with the regular bands. This transition contains both even and odd lines that are significantly more dense than the regular and sequence bands.

The intensities of individual lines are calculated according to equation (4). In the procedure applied here $S_{HL}|R|^2$ products are calculated from the experimental values of Einstein's coefficients, A, for the sequence bands[9, 10]:

$$S_{HL} \cdot |R|^2 = A \frac{3 h g'}{64 \pi^4 \nu^3} \qquad (6)$$

where g' is the statistical weight of the upper state. Further, Einstein's coefficients for a specified *J''* (line number) were calculated from the equations given in Ref. 10 in the form a+b *J''*;

For the hot band, the values of S_{HL} and $|R|^2$ were obtained separately. S_{HL} was calculated as:

$S_{HL}= (J'^2-1)/J$ for the R branch,

Table 2. Calculated wavenumbers of CO_2 hot band (11^10-01^11)

	Wavenumber [cm^{-1}]		Wavenumber [cm^{-1}]		Wavenumber [cm^{-1}]
R(1)C*	928.6887	P(2)C	925.5769	Q(1)	927.1336
R(1)D*	928.6907	P(2)D	925.5728		927.1367
R(2)C	929.4526	P(3)C	924.7848	Q(2)	927.1187
R(2)D	929.4546	P(3)D	924.7776		927.1278
R(3)C	930.2107	P(4)C	923.9872	Q(3)	927.0962
R(3)D	930.2122	P(4)D	923.9761		927.1144
R(4)C	930.9634	P(5)C	923.1836	Q(4)	927.0663
R(4)D	930.9631	P(5)D	923.1685		927.0967
R(5)C	931.7102	P(6)C	922.3745	Q(5)	927.0289
R(5)D	931.7080	P(6)D	922.3542		927.0745
R(6)C	932.4514	P(7)C	921.5601	Q(6)	926.9839
R(6)D	932.4468	P(7)D	921.5337		927.0478
R(7)C	933.1870	P(8)C	920.7397	Q(7)	926.9316
R(7)D	933.1787	P(8)D	920.7075		927.0167
R(8)C	933.9167	P(9)C	919.9138	Q(8)	926.8717
R(8)D	933.9048	P(9)D	919.8745		926.9811
R(9)C	934.6409	P(10)C	919.0825	Q(9)	926.8043
R(9)D	934.6245	P(10)D	919.0354		926.9410
R(10)C	935.3596	P(11)C	918.2454	Q(10)	926.7294
R(10)D	935.3379	P(11)D	918.1902		926.8966
R(11)C	936.0725	P(12)C	917.4026	Q(11)	926.6471
R(11)D	936.0447	P(12)D	917.3386		926.8477
R(12)C	936.7795	P(13)C	916.5542	Q(12)	926.5572
R(12)D	936.7454	P(13)D	916.4805		926.7943
R(13)C	937.4810	P(14)C	915.7002	Q(13)	926.4598
R(13)D	937.4397	P(14)D	915.6162		926.7364
R(14)C	938.1765	P(15)C	914.8408	Q(14)	926.3549
R(14)D	938.1274	P(15)D	914.7458		926.6741
R(15)C	938.8667	P(16)C	913.9753	Q(15)	926.2426
R(15)D	938.8088	P(16)D	913.8691		926.6073
R(16)C	939.5510	P(17)C	913.1047	Q(16)	926.1226
R(16)D	939.4841	P(17)D	912.9861		926.5361
R(17)C	940.2297	P(18)C	912.2283	Q(17)	925.9952
R(17)D	940.1531	P(18)D	912.0969		926.4603
R(18)C	940.9023	P(19)C	911.3462	Q(18)	925.8602
R(18)D	940.8154	P(19)D	911.2014		926.3801
R(19)C	941.5696	P(20)C	910.4585	Q(19)	925.7177
R(19)D	941.4714	P(20)D	910.2996		926.2955
R(20)C	942.2310	P(21)C	909.5654	Q(20)	925.5676
R(20)D	942.1211	P(21)D	909.3914		926.2063
R(21)C	942.8867	P(22)C	908.6665	Q(21)	925.4100
R(21)D	942.7642	P(22)D	908.4771		926.1126

Table 2. Calculated wavenumbers of CO_2 hot band (continued)

R(22)C	943.5364	P(23)C	907.7620	Q(22)	925.2448
R(22)D	943.4009	P(23)D	907.5564		926.0145
R(23)C	944.1804	P(24)C	906.8516	Q(23)	925.0721
R(23)D	944.0313	P(24)D	906.6292		925.9118
R(24)C	944.8186	P(25)C	905.9358	Q(24)	924.8918
R(24)D	944.6550	P(25)D	905.6960		925.8047
R(25)C	945.4512	P(26)C	905.0144	Q(25)	924.7040
R(25)D	945.2725	P(26)D	904.7563		925.6930
R(26)C	946.0779	P(27)C	904.0874	Q(26)	924.5085
R(26)D	945.8833	P(27)D	903.8103		925.5768
R(27)C	946.6990	P(28)C	903.1545	...	...
R(27)D	946.4875	P(28)D	902.8582		
R(28)C	947.3140	P(29)C	902.2166		
R(28)D	947.0857	P(29)D	901.8994		
R(29)C	947.9233	P(30)C	901.2725		
R(29)D	947.6770	P(30)D	900.9348		
R(30)C	948.5266	P(31)C	900.3228		
R(30)D	948.2620	P(31)D	899.9636		
R(31)C	949.1243	P(32)C	899.3674		
R(31)D	948.8406	P(32)D	898.9858		
R(32)C	949.7158	P(33)C	898.4067		
R(32)D	949.4124	P(33)D	898.0022		
R(33)C	950.3020	P(34)C	897.4399		
R(33)D	949.9778	P(34)D	897.0120		
R(34)C	950.8818	P(35)C	896.4678		
R(34)D	950.5364	P(35)D	896.0154		
R(35)C	951.4558	P(36)C	895.4897		
R(35)D	951.0886	P(36)D	895.0122		
R(36)C	952.0242	P(37)C	894.5061		
R(36)D	951.6340	P(37)D	894.0029		
R(37)C	952.5864	P(38)C	893.5171		
R(37)D	952.1729	P(38)D	892.9873		
R(38)C	953.1428	P(39)C	892.5220		
R(38)D	952.7053	P(39)D	891.9651		
R(39)C	953.6931	P(40)C	891.5215		
R(39)D	953.2310	P(40)D	890.9365		
R(40)C	954.2378	P(41)C	890.5151		
R(40)D	953.7500	P(41)D	889.9016		

* "C" and "D" refer to $11^10C \leftrightarrow 01^11C$ and $11^10D \leftrightarrow 01^11D$ transitions respectively[6].

$S_{HL}=J'(J'+2)/(J'+1)$ for the P branch ,

$S_{HL}=(2J'+1)/[J'(J'+1)]$ for the Q branch [11].

J' is the rotational quantum number of the upper state. The value for $|R|^2$ was taken from Ref. 12 as $|R|^2=7.73\ 10^{-47}$ Jcm^3 for all hot band lines. Numerical values of the internal partition functions of carbon dioxide at different temperatures, were calculated as:

$$Q=42.0966+0.4949T+8.9620\cdot10^{-4}T^2+3.9544\cdot10^{-7}T^3+1.0062\cdot10^{-9}T^4 \qquad (7)$$

Values of Eq. (7) were obtained by fitting to partition function values vs. temperature, as taken from Ref. 13.

The calculated intensities of individual sequence lines are ca. 50 times lower than the intensities of the regular bands at the same temperature[1] . At this temperature regular bands are at their maximum[1], and the so-called sequence laser is made so that the lines of the transition $[10^00,02^00]_{I,II}$ - 00^01 are absorbed by a cell at around 600 K [2-4]. Line intensities of the P and R branches of the hot band have also been calculated, and their values are by an order of magnitude higher than the intensities of the sequence bands under study, while the intensities of the lines in the Q branch decrease rapidly with increasing J.

Fig. 2 presents the temperature dependence of S for two lines of the hot band and four lines of the sequence band, arbitrarily selected. The temperature dependences show that the absorptions increase to a certain value and then decrease, with maxima situated at different points for different bands. Hot band lines have a sharper rise, reaching the maxima at about 850 K. Sequence bands rise much slower, since they correspond to transitions between higher levels, not much populated at lower temperatures. Their intensities reach maximum values at the end of the temperature range shown in the diagram, around 1200K.

The second part of this paper deals with interferences of the lines of different transitions that lie close to each other. It was necessary to calculate the absorption

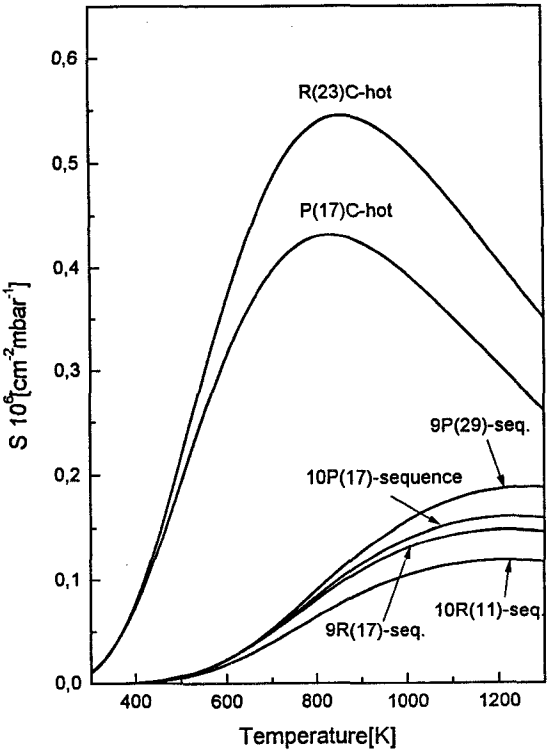

Figure 2. Temperature dependence of line intensities of some hot and sequence lines

coefficient as a function of the wavenumber for regions of interference. As seen from the theoretical procedure described above, the absorption coefficient can be calculated if the integrated intensity of absorption, Eq. (4), and the shape function,

$$k(\nu) = S \bullet \frac{b_L}{\pi[(\nu - \nu_0)^2 + b_L^2]} \qquad (8)$$

Eq. (5), are known for the conditions applied.

The above procedure was additionally employed to obtain line absorption

coefficients, k(ν), which are directly comparable to the experimental PA signals[1]. The system of calculation developed here allows the k(ν) values to be obtained for any line at any temperature.

The total coefficient of absorption is obtained as the sum of individual ones:

$$k(\nu) = k(\nu)_{reg} + k(\nu)_{hot\text{-}C} + k(\nu)_{hot\text{-}D} + k(\nu)_{seq} + \ldots \qquad (9)$$

The b_L values for pressure p and temperature T were obtained from the corresponding values expressed per unit pressure at 294 K, b_{L0}:

$$b_L = b_{L0}\, p\, \left(\frac{T}{294}\right)^{-1/2} \qquad (10)$$

where the b_{L0} values for regular band lines were obtained from Ref. 9. In the present work we assumed the b_{L0} value to be the same for all the considered adjacent lines from the hot, sequence, and regular bands. Although that parameter may slightly differ from line to line[9], this can be neglected in the present case. Actually, rough estimates given in theories[16] treat this quantity only as a function of molecular mass, collision diameter, temperature, and pressure.

Equation (8) shows that the absorption coefficient for a particular line, $k(\nu)$ is a function of pressure, temperature, and offset from the line center. All lines of these transitions whose centers are not more than 0.25 cm^{-1} apart were published previously [1]. This distance criterion is based on the 1 atm. half-width of the line. The lines 10P(20)(ν_0=944.1973cm^{-1}) (regular band) and R(23)C (ν_0=944.1804cm^{-1}), and R(23)D (944.0313cm^{-1}) of the hot band and were chosen here as appropriate to illustrate a possible interference (or contribution to mixed absorption) in conditions of varying pressure and temperature, since their centers are very close to each other.

The spectrum of interference as a function of temperature for constant pressure (100 mbar) conditions is presented in Figure 3. Line 10P(20) is clearly visible, with R(23)C at its near left and R(23)D at its far left. The latter has practically no effect

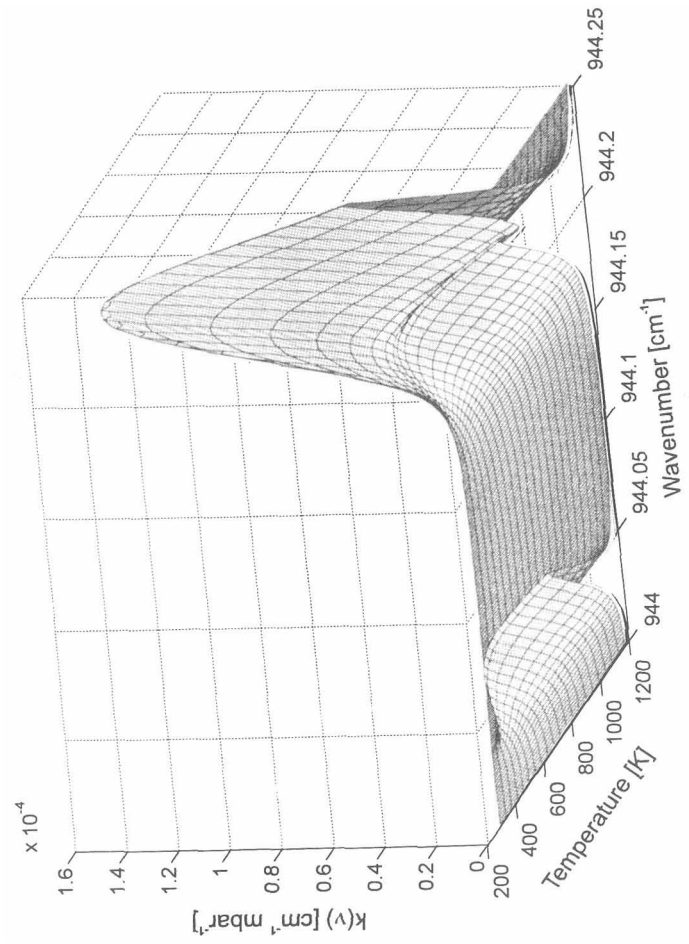

Figure 3. The spectrum of interference as a function of temperature for line 10P(20)-regular bands, R(23)C and R(23)D - hot band for constant pressure (100 mbar)

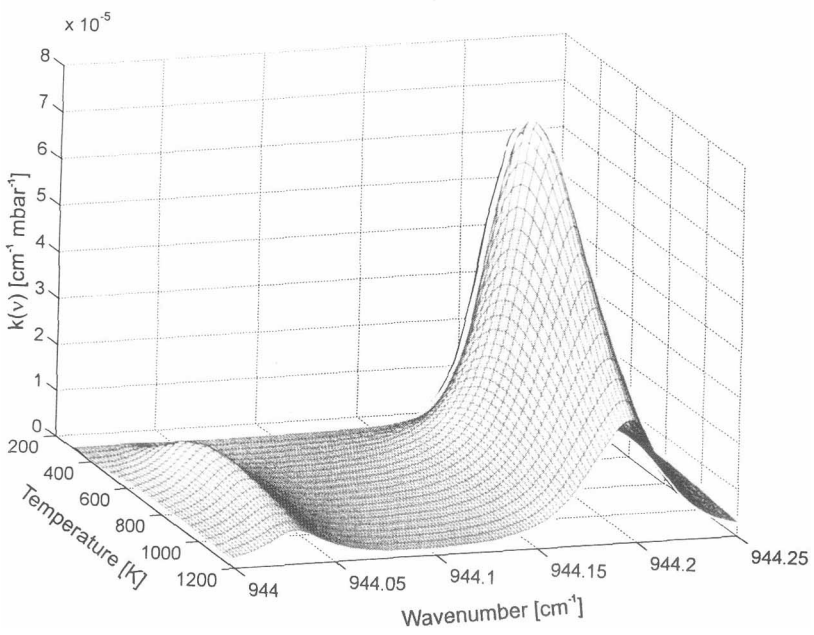

Figure 4. The spectrum of interference as a function of temperature for line 10P(20)-regular bands, R(23)C and R(23)D - hot band, for constant volume (p_i = 100 mbar)

on the total absorption coefficient of 10P(20). If p=const., or if the pressure changes are not associated with temperature changes, b_L depends on $T^{-1/2}$.

The same lines, i.e. the same frequency range, is presented in Fig. 4, but under conditions of constant volume (closed cell) with varying pressure, where the number of absorbing molecules remains the same. Under these conditions, assuming ideal gas, b_L is proportional to $T^{1/2}$, and can be calculated as:

$$b_L = b_{L0} \cdot p_i \left(\frac{T}{294}\right)^{1/2} \qquad (11)$$

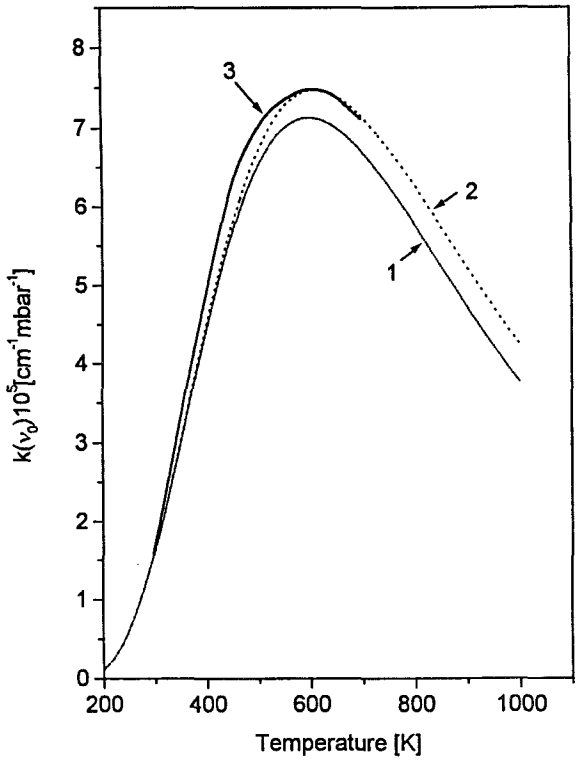

Figure 5. Temperature dependence of the absorption coefficient, p_i=100 mbar
1 - calculated 10P(20) line (regular bands); 2 - calculated 10P(20) line (reg. bands) + R(23)C line (hot band); 3 - corrected PA data

where p_i is the initial pressure (before heating). In this way, larger line broadening occurs and complete blending of line 10P(20) and line R(23)C, while line R(23)D is still separated. The initial pressure in this case is 100 mbar. It is also evident that the maximum value of the absorption coefficient at line center $k(v_0)$ in this case is significantly lower than under conditions of constant pressure, when the line is narrower.

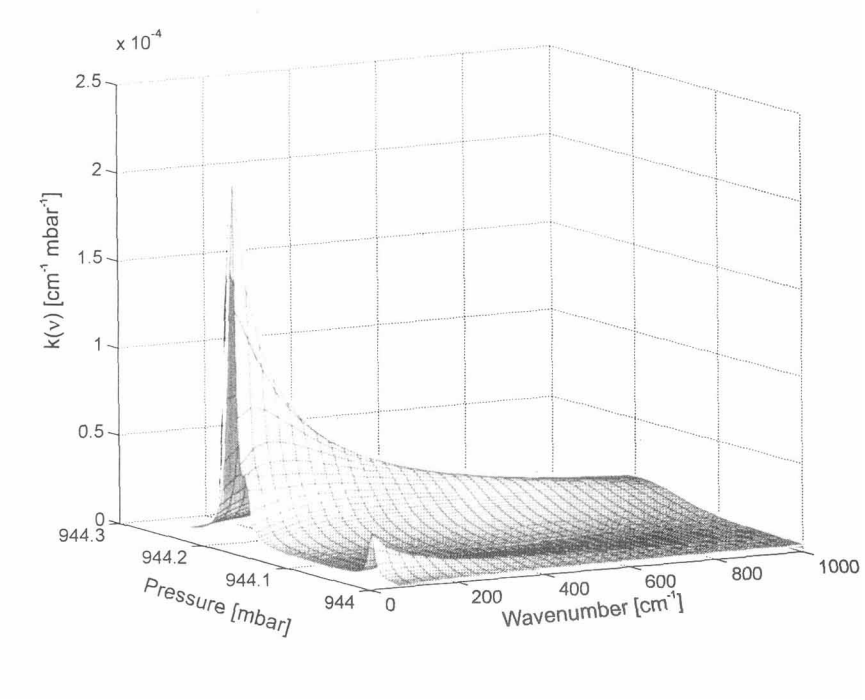

Figure 6. The spectrum of interference as a function of pressure for line 10P(20)-regular bands, R(23)C and R(23)D - hot band for constant temperature (600K)

Figure 5 represents absorption coefficient at the same conditions as the Figure 4 bat only for $\nu = \nu_0 = 944.1973$ cm^{-1}, i.e., line center for 10P(20) of the regular band. The Curve 1 in Fig. 5 is the calculated absorption coefficient, $k(\nu_0)$, as a function of temperature only. Curve 2 is the sum absorption coefficient at the *same* frequency calculated with contributions from both 10P(20) and the hot band R(23)C line. The increasing temperature increases the contribution of the hot band line, due to the relatively higher population of the upper states with temperature on the one hand and the greater interference due to line broadening.

This two band interference was experimentally recorded by a temperature controlled photoacoustic (PA) cell[1]. Generally, the PA signal is proportional to the absorption coefficient, but it is also dependent on the acoustic factors specific to each cell, which complicates its interpretation with varying pressure. The PA results are therefore corrected for these acoustic contributions using a PA measurement of pure CO_2 as a function of pressure and constant temperature[17]. Curve 3 presents the experimentally obtained and corrected values of PA signal, normalized to the corresponding calculated values $k(\nu_0)$ at 300K. Very good agreement between the experimental and the theoretical values is obtained.

The case at conditions of constant temperature (with varying pressure) is presented in Figure 6. It is clear that lines occur separately at lower pressures: 10P(20) of the regular band as the strongest, and R(23)C and R(23)D, separately. The increasing pressure causes the lines to blend together: lines 10P(20) and R(23)C first, and then all three. It can also be observed that the maximum of the absorption coefficient vs. pressure is shifted towards higher pressures for frequencies away from the line center.

CONCLUSION

The approach developed in this work represents an additional analysis of carbon-dioxide spectra in the 9-11 μm region at elevated temperatures. It predicts the general behavior of the absorption in a wide temperature range.

ACKNOWLEDGEMENT

This work was supported by the Science Funds of the Republic of Serbia and the Federal Republic of Yugoslavia.

REFERENCES

1. Lj. T. Petkovska, M. S. Trtica, M. M. Stoiljkovic' , G. S. Ristic' and . S. Miljanic' , J. Quant. Spectrosc. Radiat. Transfer 54 (1995) 509.

2. T. K. Ho, S. Y. Shaw and J. T. Shy, Appl. Phys. B 61 (1995) 95.

3. F. O. Shimizu, K. Kawai, H. Homma and A. Minoh, Jpn. J. Appl. Phys. 35 (1996) 6084.

4. F. O. Shimizu, R. Osano, T. Hirata, K. Kawai and A. Minoh, Jpn. J. Appl. Phys. 33 (1994) 6564.

5. G. Herzberg, Molecular Spectra and Molecular Structure, II. Infrared and Raman Spectra of Polyatomic Molecules (Van Nostrand, New York, 1962).

6. A. Chedin, J. Mol. Spectrosc. 76 (1979) 430.

7. L. A. Pugh and K. N. Rao, Intensities from Infrared Spectra, Molecular Spectroscopy: Modern Research, Vol. II, Ed. K. N. Rao (Academic Press, New York, 1976).

8. V. V. Nevdakh, Kvantovaya Elektron. 11 (1984) 1622.

10. V. V. Nevdakh, Infrared Phys. 25 (1985) 743.

11. G. Herzberg, Molecular Spectra and Molecular Structure, I. Spectra of Diatomic Molecules (Van Nostrand Reinolds Comp., New York, 1950).

12. C. Cousin, C. Rosseti and C. Mryer, Competes rendus 268 (1969) 1640-Serie B.

13. L.D.Gray and J.E. Selvidge, J. Quant. Spectrosc. Radiat. Transfer 5 (1965) 291.

14. P. Bunker and D. Papousek, J. Mol. Spectrosc. 32 (1969) 419.

15. J. M. Brown, J. T. Hougen, K. P. Huber, J. W. C. Johns, I. Kopp, H. Lefevre-Brion, A. J. Merer, J. Mol. Spectrosc. 55 (1975) 500.

16. A. Guillory, Introduction to Molecular Spectroscopy and Gas Emissivities (Addison-Wesley, Reading, 1959).

17. B. B. Radak, I. Pastirk and G. S. Ristic', Lj. T. Petkovska, Infrared Phys. Technol. 39/1 (1998) 7.

Date Received: March 1, 1999
Date Accepted: December 10, 1999